

R.M. Balabai, M.V. Naumenko

## Synergistic Properties of $\beta$ -Ga<sub>2</sub>O<sub>3</sub> Nanowire Arrays

Kryvyi Rih State Pedagogical University, Kryvyi Rih, Ukraine, [nikemar13@gmail.com](mailto:nikemar13@gmail.com)

Using the methods of electron density functional and *ab initio* pseudopotential, the spatial distributions of valence electron density, the density of electronic states, and Coulomb potentials along the specified directions within the arrays of  $\beta$ -Ga<sub>2</sub>O<sub>3</sub> nanowires with different cross-sectional shapes and positions in arrays were calculated. Synergistic properties of arrays of wires are established. The degree of influence of the wires on each other is determined depending on the geometric parameters of their mutual location in the array. The electronic characteristics of the array of wires as a whole are determined.

**Keywords:**  $\beta$ -Ga<sub>2</sub>O<sub>3</sub>, nanowire arrays, electron density functional, *ab initio* pseudopotential, valence electron density distribution, electron state density distribution, Coulomb potential, synergistic properties.

Received 10 October 2022; Accepted 17 February 2023.

### Introduction and formulation of the problem

Today, nanotubes and nanowires are successfully grown from various materials [1-16] and attract attention due to their mesoscopic phases, which provide them with new physical properties for use in devices [17]. Efforts have been made to fabricate  $\beta$ -Ga<sub>2</sub>O<sub>3</sub> nanotubes, but the reported [18] nanotubes were mostly disordered or bent.

Growing large-scale arrays of  $\beta$ -Ga<sub>2</sub>O<sub>3</sub>-based cylindrical structures with uniform morphology is still a huge challenge. At this point, there are few reports on the fabrication of  $\beta$ -Ga<sub>2</sub>O<sub>3</sub> nanowire arrays by inductively coupled plasma etching [19-27]; the nanowires synthesized using the chemical vapor deposition technique using hydrogen [28]; the monoclinic, vertically oriented  $\beta$ -Ga<sub>2</sub>O<sub>3</sub> nanowires obtained by hydrothermal method and annealed [29] (Fig. 1).

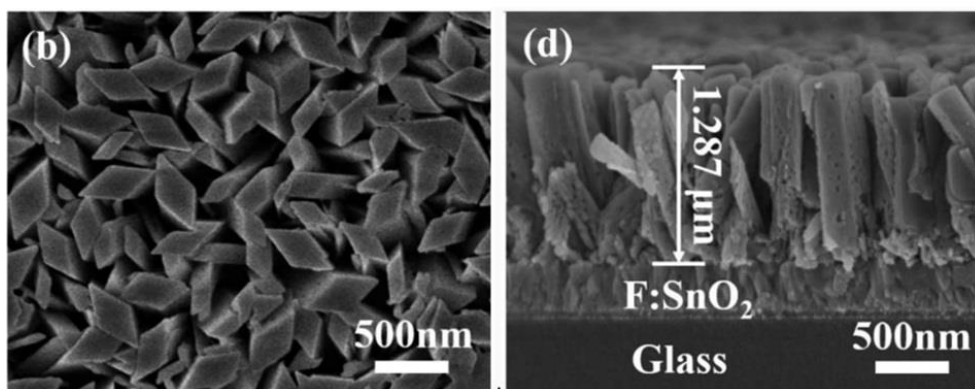


**Fig. 1.** Scanning electron microscope image at high magnification of vertically aligned arrays of  $\beta$ -Ga<sub>2</sub>O<sub>3</sub> nanowires grown on a glass substrate coated with tin oxide with fluorine impurities (left - top view), and a cross-section of the nanowire array (right) [29].

Johnson et al. [30] improved the vapor–liquid–solid growth method for the synthesis of indium oxide, gallium oxide, and tin oxide nanowires by using chemical vapor transport with gold nanoparticles as catalysts. They managed to synthesize single-crystal nanowires with a diameter of 40-100 nm and a length of more than 10-100 microns.

Alkhalayli et al. [31] analyzed the characteristic structure and morphology of  $\beta$ -Ga<sub>2</sub>O<sub>3</sub> nanowires for their application in UV photodetectors. Nanowires have a large surface area, small diameter, intrinsic scattering, and high photoconductivity, enabling UV photodetectors to achieve high sensitivity. Also, nanowires minimize the effects of lattice defects and thermal mismatch during the growth process, simplifying high-performance devices' production. In addition, one of the advantages of using nanowires is the ability to enhance light absorption and confine light to increase photosensitivity.

Due to their structural features and potential quantum confinement effects, unique electrical and optical properties are realized in semiconductor nanowires and nanotubes. Matt Low et al. [32], Hao Zeng et al. [33] believe that these semiconductor nanostructures are important elements in a wide range of promising applications for nanoscale devices due to their wide range of compositions and band structures. Current research focuses on rational synthetic control of one-dimensional nanoscale building blocks, novel property characterization and device fabrication based on nanowire building blocks, and integration of nanowire elements into complex functional architecture.

A comprehensive understanding of the synergistic relationship between the structural morphology of  $\beta$ -Ga<sub>2</sub>O<sub>3</sub> nanowire arrays and the electronic properties of the array as a whole is necessary. Our work is devoted to the numerical determination of the characteristics of the electronic subsystem of model arrays of  $\beta$ -Ga<sub>2</sub>O<sub>3</sub> nanowires of various cross-sections and packing geometries. The main research methods were electron density functional and *ab initio* pseudopotential theories. Using the author's program [34], the spatial distributions of the density of valence electrons, distributions of the density of electronic states, and Coulomb potentials along the specified directions within the array of nanowires were calculated.

## I. Models and calculation methods

The numerical experiments from the first principles were performed according to the algorithm described in works [35-37]. Since the calculation algorithm assumed translational symmetry in the studied atomic system, an artificial superlattice of the orthorhombic type was first created. The symmetry of the superlattice made it possible to match the Cartesian system to the crystallographic one. The objects of the study determined the parameters of the unit cell of the superlattice and the atomic basis. The objects of the calculation were infinite arrays of  $\beta$ -Ga<sub>2</sub>O<sub>3</sub> nanowires of different diameters, the same height, and different cross-sectional shapes: cylindrical and parallelogram. The wires were located relative to each other with respect to rectangular symmetry.

The ground states of the subsystem of valence electrons of model arrays of nanowires were determined using the self-consistent solution of the Kohn-Sham equations in the local approximation with fixed atomic cores. The calculations were performed under the following conditions: the integration over the Brillouin zone of the artificial superlattice was replaced by the calculation at the  $\Gamma$ -point; self-alignment iterations stopped if the calculation results of the current iteration coincided with the previous one with a predetermined error, their number varied depending on the object being calculated, but usually our results converged after 3-6 iterations; Kohn-Sham wave functions should be written in the form of Bloch functions, expanded on the basis of plane waves; the number of plane waves in the distribution of the wave function was reduced by means of trial calculations and assessment of the physicality of the obtained results (spatial distribution of the electron density, the size of the gap in the energy electronic spectrum between the last occupied state and the first unoccupied one, general ideas about the modeled nanostructure or evaluation of the obtained results in comparison with the results, obtained by other authors), the number of plane waves was chosen to be approximately 20-25 waves per one base atom; the atomic basis was not optimized; the interaction of valence electrons with ionic cores was processed using a pseudopotential from the first principles of Bechelet-Hemann-Schleter.

The synergistic properties of the electronic subsystem of the array of wires were studied, that is, the degree of influence of the wires on each other was determined depending on the geometric parameters of their mutual location in the array and the electronic characteristics of the array of wires as a whole. The influence of the possible growth substrate of the array of wires was not taken into account.

The corresponding values of the parameters of the unit cell of the superlattice and the coordinates of atoms in the basis allowed us to model infinite arrays of  $\beta$ -Ga<sub>2</sub>O<sub>3</sub> wires. On Fig. 2 images from different angles of numerically reproduced cylindrical nanowires are given. The nanowires periodically arranged in the XY plane, they have a height equal to  $h = 1.57$  nm, different diameters  $2 \cdot R$  (0.61 or 0.95 nm, "thin" or "thick"). The nanowires separated by a vacuum and located relative to each other one according to square symmetry at variable distances  $r$  (the distance between the centers of the cylinders is marked as "a" in the figure). Wires in the form of a cylinder had a symmetrical cross-section – a circle, other types of wires - prism-shaped - had spatial angles between the limiting faces and the dimensions of the faces corresponding to the monoclinic  $\beta$ -Ga<sub>2</sub>O<sub>3</sub> syngonia.

The parameter "c" (Z direction) of the unit cell of the superlattice was chosen so as to avoid the interaction between the atoms of the nanowire array translating in the Z direction, while the interaction in the X, Y directions was detected. The number of atoms in the base was 60 atoms for thin cylindrical and prismatic wires, and 120 atoms for thick cylindrical wires.

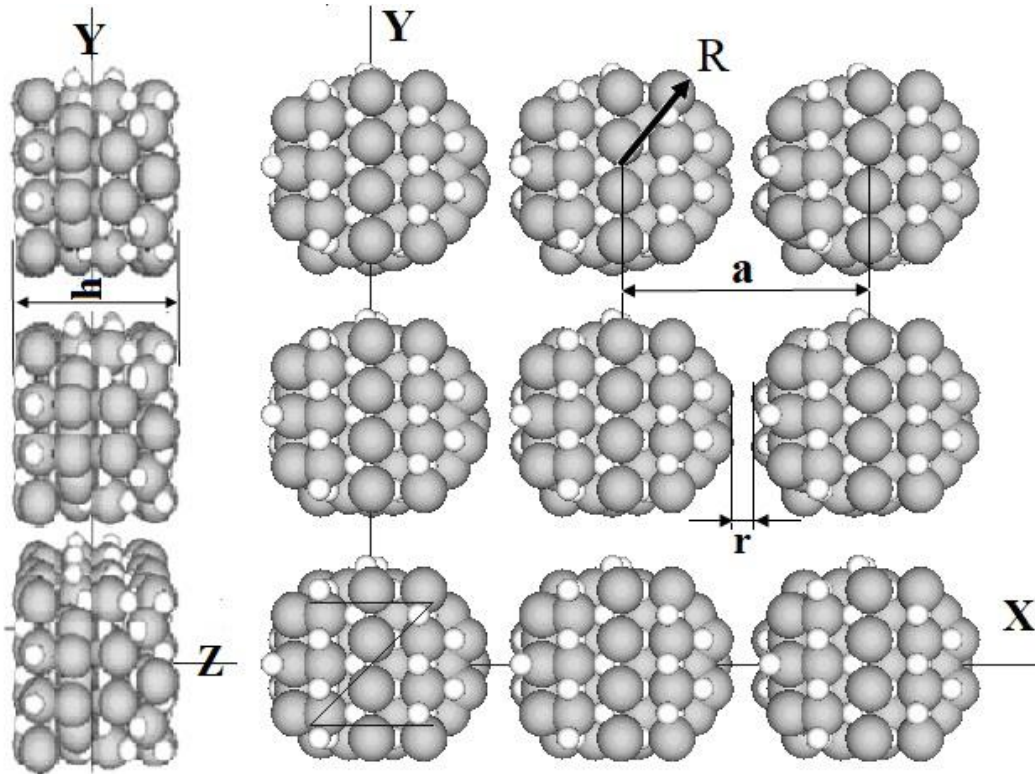


**Fig. 2.** Fragments of an infinite array of  $\beta$ -Ga<sub>2</sub>O<sub>3</sub> wires. Thick nanowires are shown in different angles: on the left – in the ZY plane, on the right – in the XY plane. Gray spheres are Ga atoms, white spheres are O atoms.

## II. Results and discussion

To determine the quantitative characteristics of the interaction between nanowires in the array due to long-range electric forces, Coulomb potentials induced by valence electrons were calculated along different directions of nanowire arrays (Fig. 3). As a sign that the interaction between the electronic subsystem of the wires disappears, we considered the equality of the Coulomb potential to be zero in the region between the wires.

It was established that the interaction between the cylindrical wires is manifested starting from the distance between them from 0.71 nm for thin wires, from 0.37 nm for thick ones (Fig. 4-5

An obvious increase in the values of the Coulomb

potentials induced by the electronic subsystem was observed when the wires in the array approached each other. At the same time, this growth occurred more intensively for thin wires. The similarity of the change in the Coulomb potentials, calculated in different directions of the array of cylindrical wires, and the closeness of their numerical values indicate the isotropic nature of the electrical properties of the array, and some difference is associated with an irregular circle in the cross-section of the wire and with different types of atoms lining its side surface. An increase in the values of the Coulomb potentials, induced by the electronic subsystem and proportional to its charge density, in the region between the wires correlates with a decrease in the intensity of the spatial distributions of the density of valence electrons inside the wires, especially this is noticeable in the array of thin wires (Fig. 6).

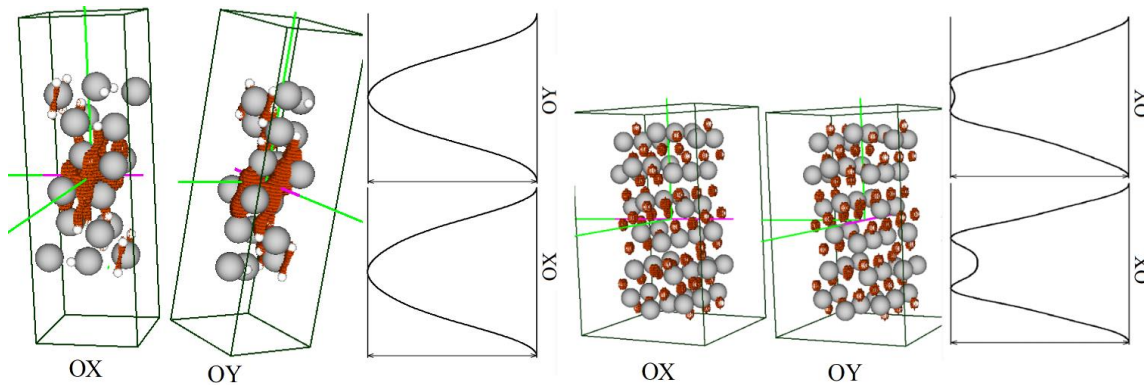


**Fig. 3.** Directions along arrays of thin (left) and thick (right) nanowires for calculating Coulomb potentials and their designation: OX, OY. A unit cell with the maximum iso-value electron density containing one wire is given; the translation operation involved in the calculation algorithm implements an infinite array of wires in the XY plane. Examples of the obtained potential distributions are given.

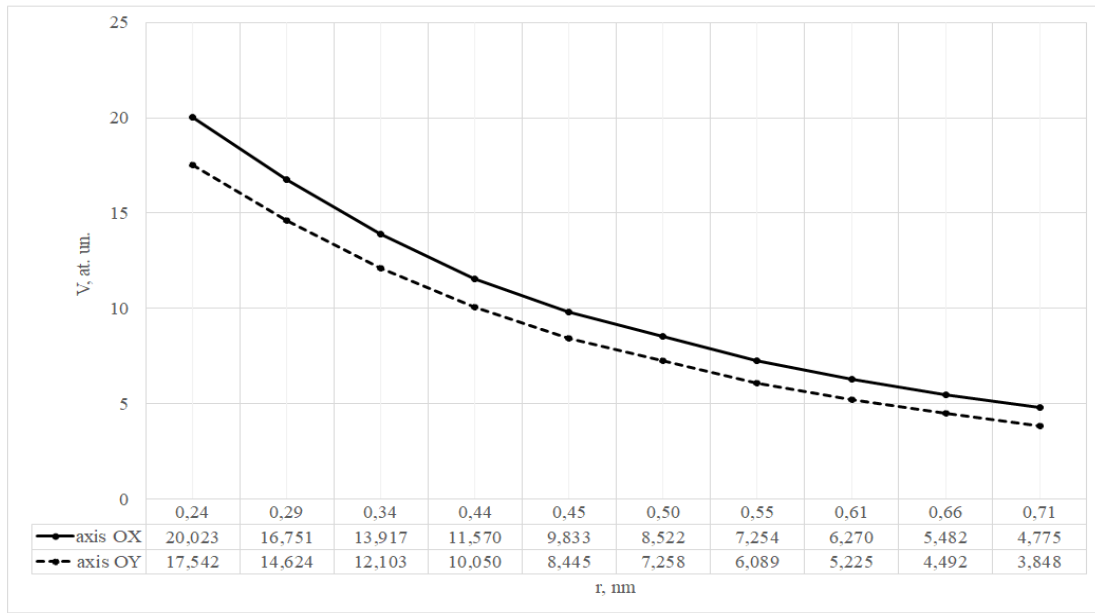


**Fig. 4.** Values of the Coulomb potentials depending on the distance between thin wires. Coulomb potentials are calculated in the middle between the wires in the directions indicated on fig. 2 in the array of wires.

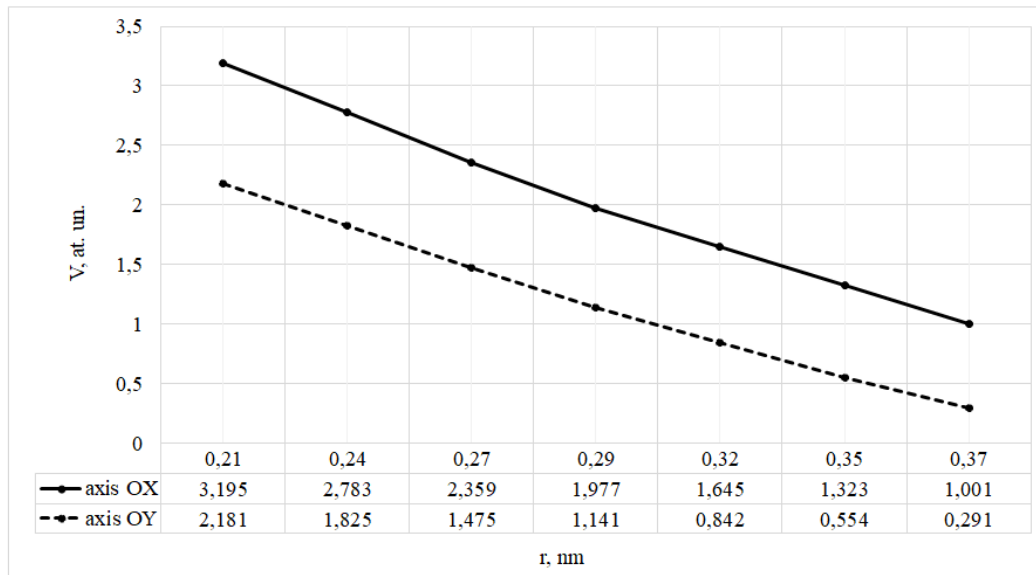


**Fig. 5.** Values of the Coulomb potentials depending on the distance between thick wires. Coulomb potentials are calculated in the middle between the wires in the directions indicated on fig. 2 in the array of wires.

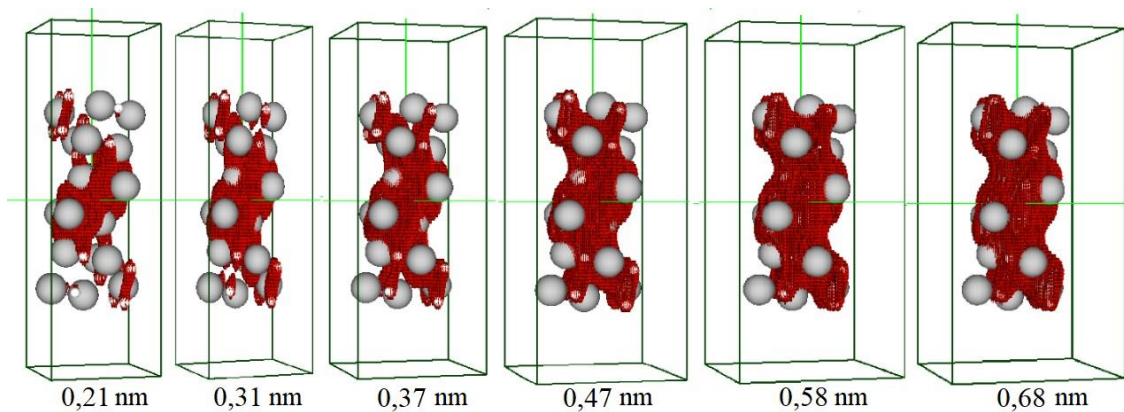


**Fig. 6.** Spatial distributions of valence electron density in the interval of iso-values 0.8-0.7 from the maximum in the array of thin  $\beta$ -Ga<sub>2</sub>O<sub>3</sub> wires when the distance between them changes from 0.21 nm to 0.68 nm.

A decrease in the width of the electronic band gap is evidence of the presence of a synergistic (collective) effect in the electronic properties of an array of closely spaced thick  $\beta\text{-Ga}_2\text{O}_3$  wires. Namely, wires located far from each other exhibit the properties of a single cluster and have a significant width of the band gap (HOMO-LUMO) - about 180 eV. Whereas closely located wires demonstrate the properties of an ordered interacting metastructure and a much smaller size of the band gap - about 40 eV (Fig. 7). At the same time, the change in the value of the band gap depending on the reduction in the distance between the wires is monotonic.

As for the array of thin wires, the nature of the change in the value of the electronic band gap depending on the distance between the wires is non-monotonic, and when the distance between them is about 0.50 nm, the value of the band gap was the largest. The rest of the obtained values were almost an order of magnitude smaller than for the array of thick wires (Fig. 8).

Arrays of prism-like wires bounded by faces

characteristic of the  $\beta\text{-Ga}_2\text{O}_3$  monoclinic syngony have anisotropic electrical properties, since, firstly, the surface area of the interacting faces of the prism wires in the OY direction is four times larger than in the OX direction and, secondly, the wires are located relative to each other according to rectangular, but not square, symmetry (Fig. 9). This fact is reflected in the distributions of Coulomb potentials (Fig. 10-11). Namely, all distributions are different in shape and numerical values. At the same time, the expected greater intensity of interaction between the faces of the wires, which have a larger area, did not come true. On the contrary, smaller potentials were fixed between these faces, which was apparently determined by incomplete atomic bonds, which were more active on the faces of a smaller area, i.e. in the OX direction. As for the values of the electronic band gap of the array of prism-shaped wires, they are non-monotonic depending on the distance between them.

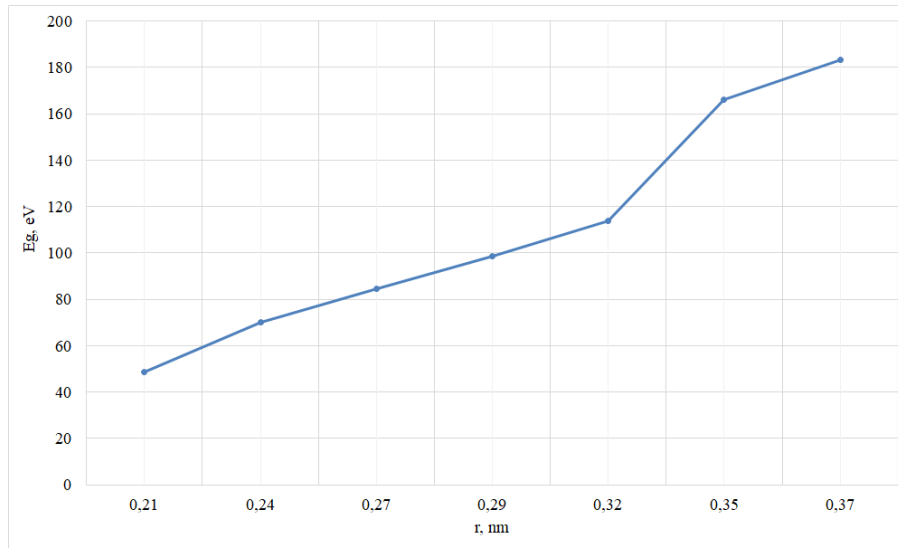


**Fig. 7.** Dependence of the width of the electronic band gap of the ordered metastructure (an array of thick cylindrical  $\beta\text{-Ga}_2\text{O}_3$  wires) on the distance between the wires.



**Fig. 8.** Dependence of the width of the electronic band gap of the ordered metastructure (an array of thin cylindrical  $\beta\text{-Ga}_2\text{O}_3$  wires) on the distance between the wires.

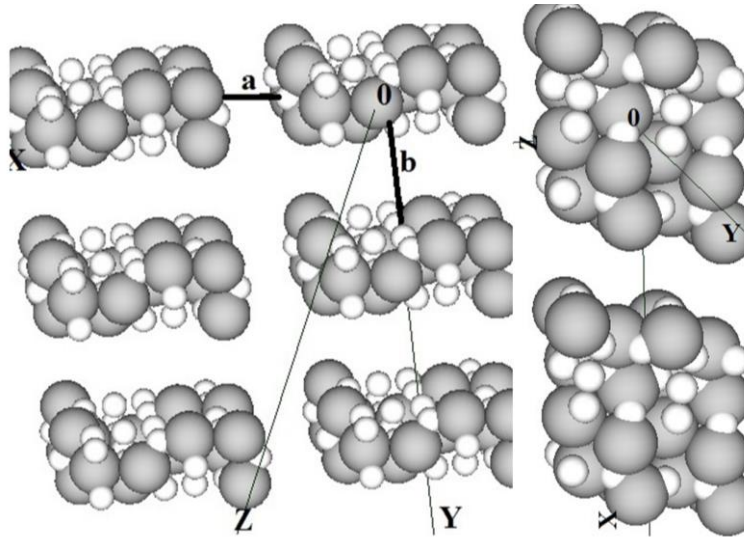


**Fig. 9.** Directions along arrays of prism-shaped nanowires bounded by faces characteristic of  $\beta$ -Ga<sub>2</sub>O<sub>3</sub> monoclinic syngonia for calculation of Coulomb potentials and their designation: OX, OY. The symbols "a", "b" indicate the distances between the wires.

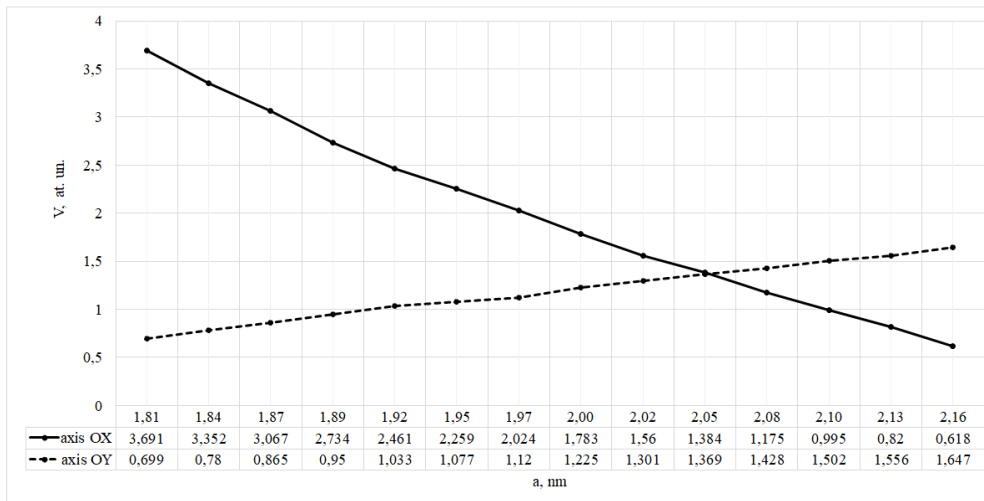


**Fig. 10.** Values of the Coulomb potentials depending on the distance between the prism-shaped wires. Coulomb potentials are calculated in the middle between the wires in the directions indicated on fig. 9 in the array of wires. The distance "a" between the wires was changed, the distance "b" was fixed at 1.8 nm.

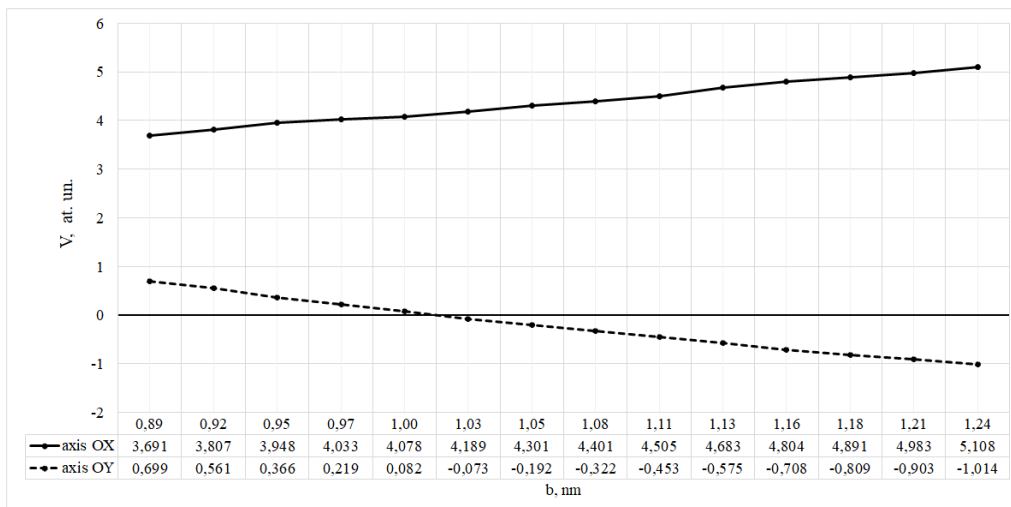


**Fig. 11.** Values of the Coulomb potentials depending on the distance between the prism-shaped wires. Coulomb potentials are calculated in the middle between the wires in the directions indicated on fig. 9 in the array of wires. The distance "b" between the wires was changed, the distance "a" was fixed at 0.9 nm.

## Conclusions

Using the methods of electron density functional theory and *ab initio* pseudopotential, the spatial distributions of the valence electron density, the distributions of the density of electronic states, and the Coulomb potentials along the specified directions within the arrays of  $\beta$ -Ga<sub>2</sub>O<sub>3</sub> nanowires of various cross-sectional shapes and positions relative to each other were calculated. Synergistic properties of arrays of wires are established, and the degree of influence of wires on each other is determined depending on the geometric

parameters of their mutual location in the array, and the electronic characteristics of the array of wires as a whole. Arrays of  $\beta$ -Ga<sub>2</sub>O<sub>3</sub> wires of cylindrical shape and larger diameter reveal more controlled and physically justified synergistic electronic characteristics than arrays of cylindrical wires of smaller diameter and prismatic shape.

**Balabai R.M.** – Doctor of Physics and Mathematics of Sciences, Professor of the Department of Physics and Methods of its Teaching;  
**Naumenko M.V.** – Student PhD of the Department of Physics and Methods of its Teaching..

- [1] B. Cheng, E. T. Samulski, *Fabrication and characterization of nanotubular semiconductor oxides In<sub>2</sub>O<sub>3</sub> and Ga<sub>2</sub>O<sub>3</sub>*, Journal of Materials Chemistry, 11, 2901 (2001); <https://doi.org/10.1039/B108167E>.
- [2] B. Zhang, P.-X. Gao, *Metal oxide nanoarrays for chemical sensing: a review of fabrication methods, sensing modes, and their inter-correlations*, Front. Mater. 6(55) (2019); <https://doi.org/10.3389/fmats.2019.00055>.
- [3] Y. Zhang, J. Yang; Q. Li, X. Cao, *Preparation of Ga<sub>2</sub>O<sub>3</sub> nanoribbons and tubes by electrospinning*, J. Cryst. Growth, 308, 180 (2007); <https://doi.org/10.1016/j.jcrysgro.2007.07.036>.
- [4] N. W. Gong, M. Y. Lu, C. Y. Wang, Y. Chen, L. J. Chen, *Au(Si)-filled  $\beta$ -Ga<sub>2</sub>O<sub>3</sub> nanotubes as wide range high-temperature nanothermometers*. Appl. Phys. Lett., 92, 073101 (2008); <https://doi.org/10.1063/1.2840574>.
- [5] H. Jiang, Y. Chen, Q. Zhou, Y. Su, H. Xiao, L. Zhu, *Temperature dependence of Ga<sub>2</sub>O<sub>3</sub> micro/nanostructures via vapor phase growth*, Mater. Chem. Phys., 103, 14 (2007); <https://doi.org/10.1016/j.matchemphys.2007.02.031>.
- [6] T. Braniste, and et al., *Aero-Ga<sub>2</sub>O<sub>3</sub> Nanomaterial Electromagnetically Transparent from Microwaves to Terahertz for Internet of Things Applications*, Nanomaterials, 10(6), 1047 (2020); <https://doi.org/10.3390/nano10061047>.
- [7] Ziyao Zhou, Changyong Lan, SenPo Yip, Renjie Wei, Dapan Li, Lei Shu, Johnny C. Ho, *Towards high-mobility In<sub>2</sub>xGa<sub>2-2x</sub>O<sub>3</sub> nanowire field-effect transistors*, Nano Research, 11 (11), 5935 (2018); <https://doi.org/10.1007/s12274-018-2106-9>
- [8] G. F. Yang, and et al. *Fabrication of GaN Nanocolumns with Semipolar Plane Using Ni nano-island masks*, Semicond. Technol., 36, 417 (2011).
- [9] H. S. Kim, G. Y. Yeom, J. W. Lee, T. I. Kim, *Characteristics of inductively coupled Cl<sub>2</sub>/BCl<sub>3</sub> plasmas during GaN etching*, J. Vac. Sci. Technol. A, 17, 2214 (1999); <https://doi.org/10.1116/1.581749>.
- [10] M. Y. Hsieh, C. Y. Wang, L. Y. Chen, M. Y. Ke, J. Huang, *InGaN-GaN nanorod light emitting arrays fabricated by silica nanomasks*, IEEE J. Quantum Electron., 44, 468 (2008); <https://doi.org/10.1109/JQE.2007.916665>
- [11] J. Lin, R. Zong, M. Zhou, Y. Zhu, *Photoelectric catalytic degradation of methylene blue by C<sub>60</sub>-modified TiO<sub>2</sub> nanotube array*, Appl. Catal. B Environ., 89, 425 (2009); <https://doi.org/10.1016/j.apcatb.2008.12.025>.
- [12] T. J. Hsueh, S. J. Chang, C. L. Hsu, Y. R. Lin, I. C. Chen, *ZnO nanotube ethanol gas sensors*, J. Electrochem. Soc., 155, K152 (2008); <https://iopscience.iop.org/article/10.1149/1.2952535>.
- [13] A. Star, Y. Lu, K. Bradley, G. Grüner, *Nanotube optoelectronic memory devices*, Nano Lett., 4, 1587 (2004); <https://doi.org/10.1021/nl049337f>.
- [14] J. Han, Z. Liu, K. Guo, B. Wang, X. Zhang, T. Hong, *High-efficiency photoelectrochemical electrodes based on ZnIn<sub>2</sub>S<sub>4</sub> sensitized ZnO nanotube arrays*, Appl. Catal. B Environ., 163, 179 (2015); <https://doi.org/10.1016/j.apcatb.2014.07.040>.
- [15] Z. Zhuang, and et al. *High color rendering index hybrid III-nitride/nanocrystals white light-emitting diodes*, Adv. Funct. Mater., 26, 36 (2016); <https://doi.org/10.1002/adfm.201502870>.
- [16] B. Liu, and et al. *Hybrid light emitters and UV solar-blind avalanche photodiodes based on iii-nitride semiconductors*, Adv. Mater., 32, 1904354 (2020); <https://doi.org/10.1002/adma.201904354>.
- [17] Y. C. Choi, and et al., *Catalytic growth of beta-Ga<sub>2</sub>O<sub>3</sub> nanowires by arc discharge*, Adv. Mater., 12 (10), [https://doi.org/10.1002/\(SICI\)1521-4095\(200005\)12:10<746::AID-ADMA746>3.0.CO;2-N](https://doi.org/10.1002/(SICI)1521-4095(200005)12:10<746::AID-ADMA746>3.0.CO;2-N).
- [18] S. Ding, L. Zhang, Y. Li, X. Xiu, Z. Xie, T. Tao, B. Liu, P. Chen, R. Zhang, Y. Zheng, *A selective etching route for large-scale fabrication of  $\beta$ -Ga<sub>2</sub>O<sub>3</sub> micro-/nanotube arrays*, Nanomaterials, 11, 3327 (2021); <https://doi.org/10.3390/nano11123327>.
- [19] H. Liang, Y. Chen, X. Xia, C. Zhang, R. Shen, Y. Liu, Y. Luo, G. Du, *A preliminary study of SF<sub>6</sub> based inductively coupled plasma etching techniques for beta gallium trioxide thin film*, Mater. Sci. Semicond. Proc., 39, 582 (2015); <https://doi.org/10.1016/j.mssp.2015.05.065>.
- [20] J. E. Hogan, S.W. Kaun, E. Ahmadi, Y. Oshima, J. S. Speck, *Chlorine-based dry etching of  $\beta$ -Ga<sub>2</sub>O<sub>3</sub>*, Semicond. Sci. Technol., 31, 065006 (2016); <https://doi.org/10.1088/0268-1242/31/6/065006>.
- [21] J. Yang, S. Ahn, F. Ren, S. Pearton, R. Khanna, K. Bevlín, D. Geerpuram, A. Kuramata, *Inductively coupled plasma etching of bulk, single-crystal Ga<sub>2</sub>O<sub>3</sub>*, J. Vac. Sci. Technol. B, 35, 031205 (2017); <https://doi.org/10.1116/1.4982714>.

- [22] Z. Lin, X. Xiu, S. Zhang, X. Hua, Z. Xie, R. Zhang, P. Han, Y. Zheng, *Arrays of GaN nano-pillars fabricated by nickel nano-island mask*, Mater. Lett., 108, 250 (2013); <https://doi.org/10.1016/j.matlet.2013.07.005>.
- [23] L. Zhang, X. Xiu, Y. Li, Y. Zhu, X. Hua, Z. Xie, T. Tao, B. Liu, P. Chen, R. Zhang, and et al. *Solar-blind ultraviolet photodetector based on vertically aligned single-crystalline  $\beta$ -Ga<sub>2</sub>O<sub>3</sub> nanowire arrays*, Nanophotonics, 9, 4497 (2020); <https://doi.org/10.1515/nanoph-2020-0295>.
- [24] S. Wang, Y. W. Li, X. Q. Xiu, and et al. *Synthesis and characterization of  $\beta$ -Ga<sub>2</sub>O<sub>3</sub>@GaN nanowires*, Chin. Phys. B, 28, 028104 (2019); <https://doi.org/10.1088/1674-1056/28/2/028104>.
- [25] T. Yamada, J. Ito, R. Asahara, K. Watanabe, M. Nozaki, S. Nakazawa, Y. Anda, M. Ishida, T. Ueda, A. Yoshigoe, and et al., *Comprehensive study on initial thermal oxidation of GaN (0001) surface and subsequent oxide growth in dry oxygen ambient*, J. Appl. Phys., 121, 035303 (2017); <https://doi.org/10.1063/1.4974458>.
- [26] J. H. Choi, M. H. Ham, W. Lee, J. M. Myoung, *Fabrication and characterization of GaN/amorphous Ga<sub>2</sub>O<sub>3</sub> nanocables through thermal oxidation*, Solid State Commun., 142, 437 (2007); <https://doi.org/10.1016/j.ssc.2007.03.034>.
- [27] L. Zhang, Y. Li, X. Xiu, G. Xin, Z. Xie, T. Tao, B. Liu, P. Chen, R. Zhang, Y. Zheng, *Preparation of vertically aligned GaN@Ga<sub>2</sub>O<sub>3</sub> core-shell heterostructured nanowire arrays and their photocatalytic activity for degradation of Rhodamine B.*, Superlattices Microstruct., 143, 106556 (2020); <https://doi.org/10.1016/j.spmi.2020.106556>.
- [28] [28] J.P. Rex and et al., *The influence of deposition temperature on the structural, morphological and optical properties of micro-size structures of beta-Ga<sub>2</sub>O<sub>3</sub>*, Results in Physics, 14, 102475 (2019); <https://doi.org/10.1016/j.rinp.2019.102475>.
- [29] W. Shunli, and et al.,  *$\beta$ -Ga<sub>2</sub>O<sub>3</sub> nanorod arrays with high light-to-electron conversion for solar-blind deep ultraviolet photodetection*, RSC Adv., 9, 6064 (2019); <https://doi.org/10.1039/c8ra10371b>.
- [30] M. C. Johnson, Shaul Aloni, D. E. McCready, E. D. Bourret-Courchesne, *Controlled vapor-liquid-solid growth of indium, gallium, and tin oxide nanowires via chemical vapor transport*, Crystal Growth & Design, 6(8), 1936 (2006); <https://doi.org/10.1021/cg050524g>.
- [31] B. Alhalaili, and et al. *Gallium oxide nanowires for UV detection with enhanced growth and material properties*, Scientific Reports, 10, 21434 (2020); <https://doi.org/10.1038/s41598-020-78326-x>.
- [32] M. Law, J. Goldberger, P. Yang, *Semiconductor nanowires and nanotubes*, Annu. Rev. Mater. Res., 34, 83 (2004); <https://doi.org/10.1146/annurev.matsci.34.040203.112300>.
- [33] Hao Zeng and at al. *Metal-oxide nanowire molecular sensors and their promises*, Chemosensors, 9(2), 41 (2021); <https://doi.org/10.3390/chemosensors9020041>.
- [34] *Ab initio calculation*. Web source: <http://sites.google.com/a/kdpu.edu.ua/calculationphysics>.
- [35] R. Balabai, M. Naumenko, *Methodology of converting of the coordinates of the basis atoms in a unit cell of crystalline  $\beta$ -Ga<sub>2</sub>O<sub>3</sub>, specified in a monoclinic crystallographic system, in the laboratory cartesian coordinates for computer applications*, Photoelectronics, 29, 12-20 (2020); <https://doi.org/10.18524/0235-2435.2020.29.225463>.
- [36] R. Balabai, V. Zdeschits, M. Naumenko, *Mechanical modification of electronic properties of ultrathin  $\beta$ -Ga<sub>2</sub>O<sub>3</sub> films*, Ukrainian Journal of Physics, 66(12), 1048 (2021); <https://doi.org/10.15407/ujpe66.12.1048>.
- [37] R. Balabai, O. Bondarenko, M. Naumenko, *Energy levels of acceptor impurities in  $\beta$ -Ga<sub>2</sub>O<sub>3</sub> nanostructures*, Materials Today: Proceedings, 62(9), 5838-5844 (2022); <https://doi.org/10.1016/j.matpr.2022.05.365>.

Р.М. Балабай, М.В. Науменко

## Синергетичні властивості масивів нанодротів $\beta$ -Ga<sub>2</sub>O<sub>3</sub>

Криворізький державний педагогічний університет, Кривий Різ, Україна, [nikemar13@gmail.com](mailto:nikemar13@gmail.com)

Методами теорії функціоналу електронної густини та *ab initio* псевдопотенціалу розраховано просторові розподіли густини валентних електронів, розподіли густини електронних станів та Кулонівські потенціали вздовж визначених напрямків у межах масивів нанодротів  $\beta$ -Ga<sub>2</sub>O<sub>3</sub> різних форм перерізу та розташування один відносно одного. Встановлені синергетичні властивості масивів дротів, визначена ступінь впливу дротів один на одного в залежності від геометричних параметрів їх взаємного розташування в масиві та електронні характеристики масиву дротів як єдиного цілого.

**Ключові слова:**  $\beta$ -Ga<sub>2</sub>O<sub>3</sub>, масиви нанодротів, функціонал електронної густини, *ab initio* псевдопотенціал, розподіл густини валентних електронів, розподіл густини електронних станів, Кулонівський потенціал, синергетичні властивості.